The location of the high-energy emission in blazars: Constraints from correlated radio and gamma-ray variability

Walter Max-Moerbeck (NRAO)
with the OVRO blazar monitoring group
and the Fermi-LAT collaboration

April 30, 2013

Blazars

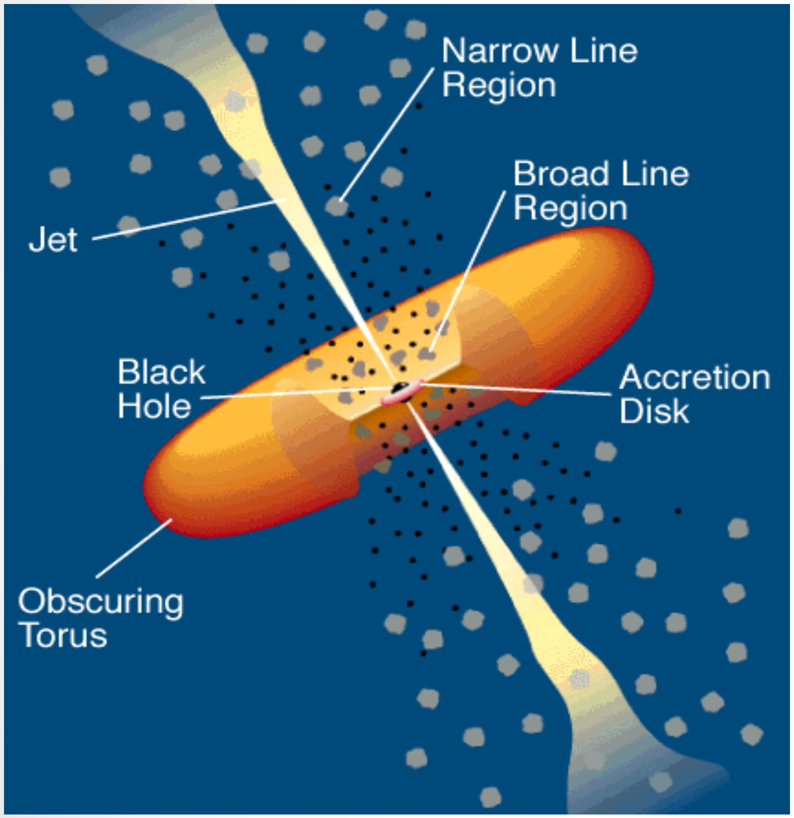

Urry and Padovani 1995

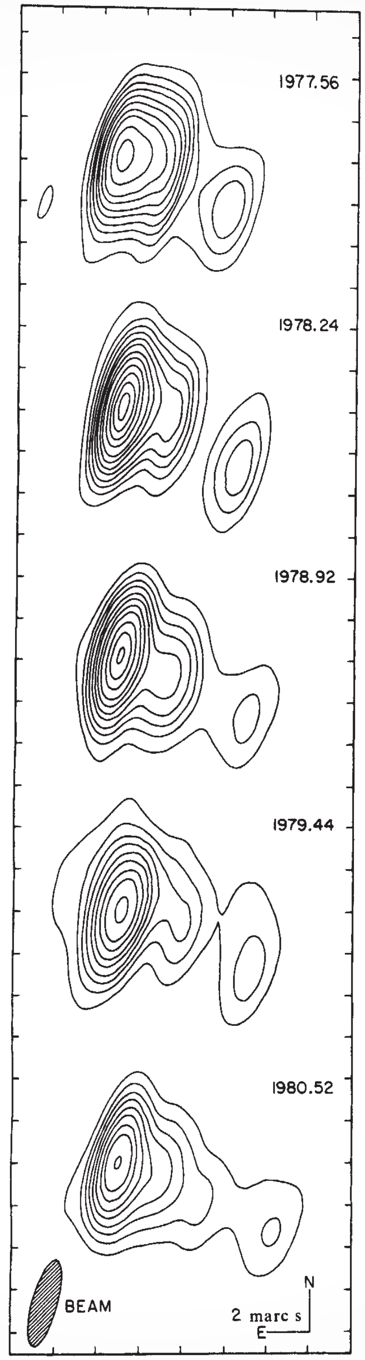

- Radio loud
- Small angular size
- Superluminal expansion

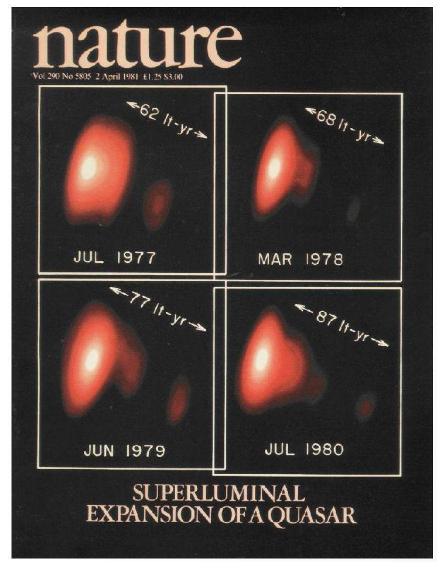

3C 273, Pearson et al. 1981

Blazars: SED

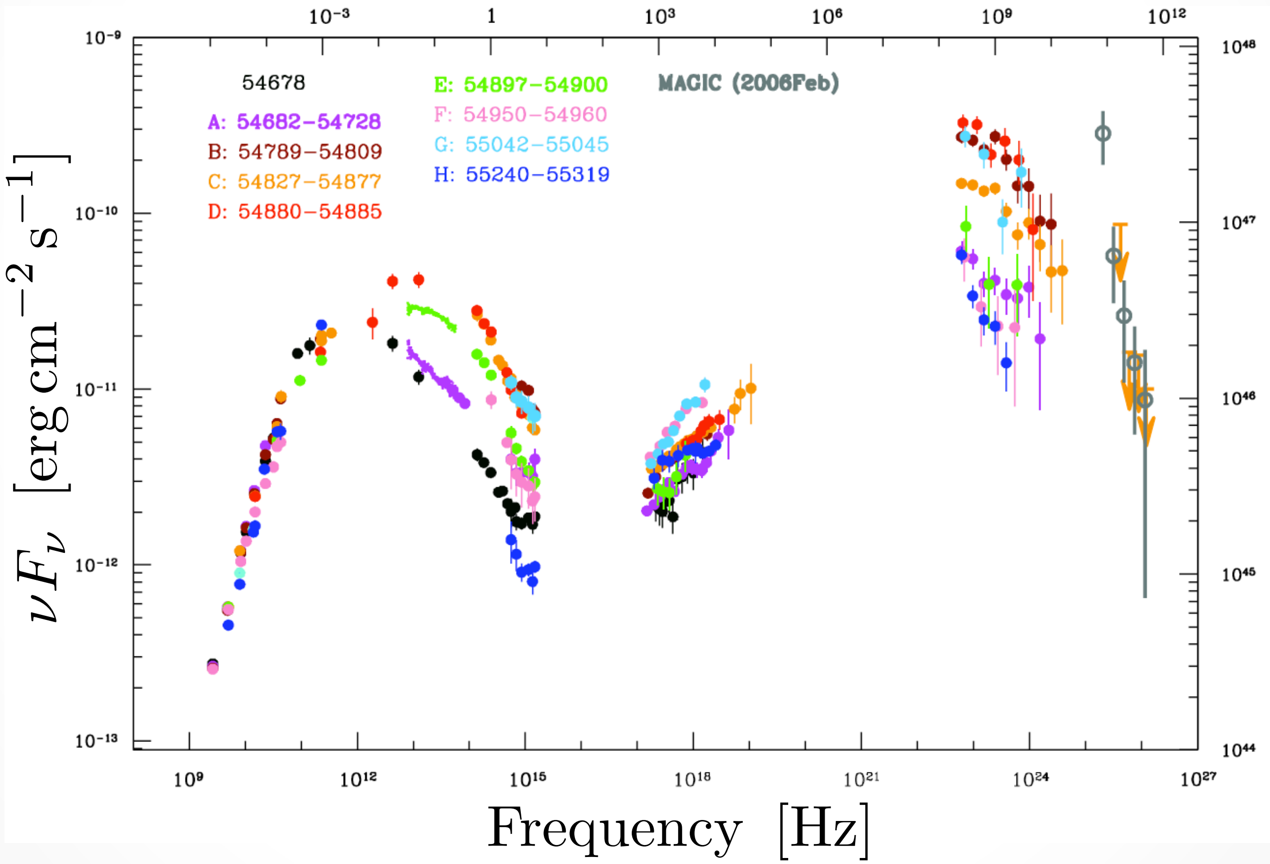

Broadband spectral energy distribution
3C 279 from Hayashida et al. 2012

Blazars: Variability

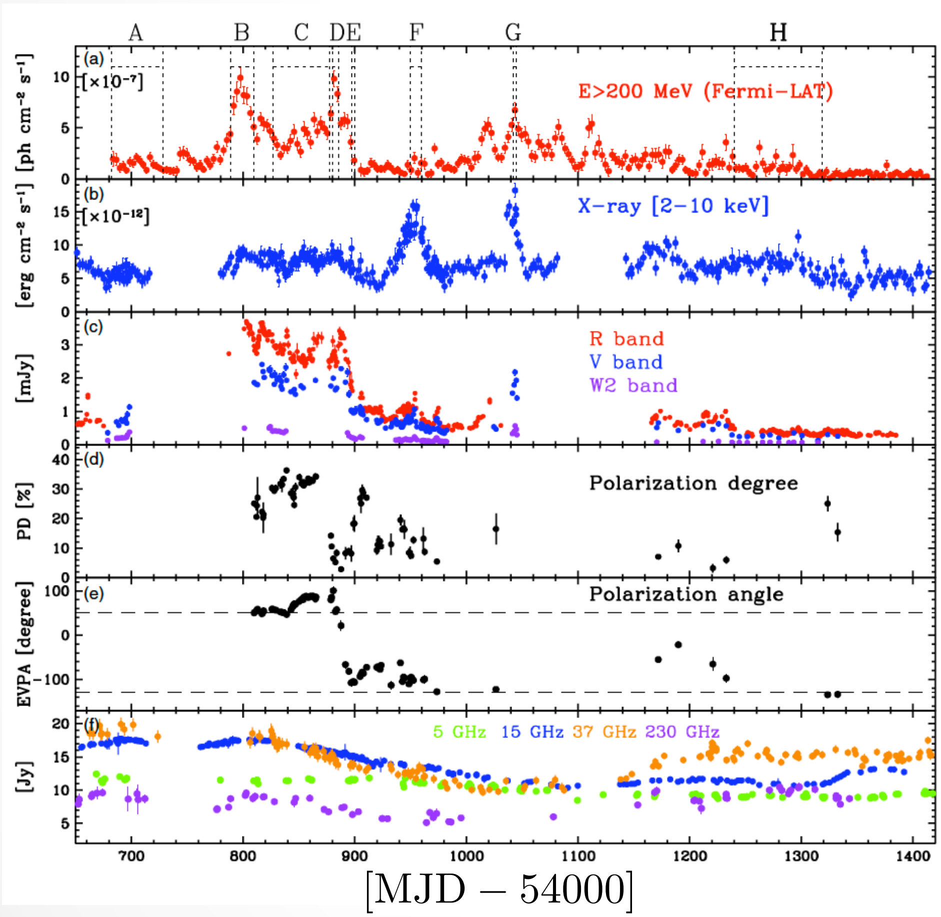

γ–ray

x – ray

optical/UV

optical polarization degree

optical polarization angle

radio mm and cm

Variability
3C 279 from Hayashida et al. 2012

Models of blazars

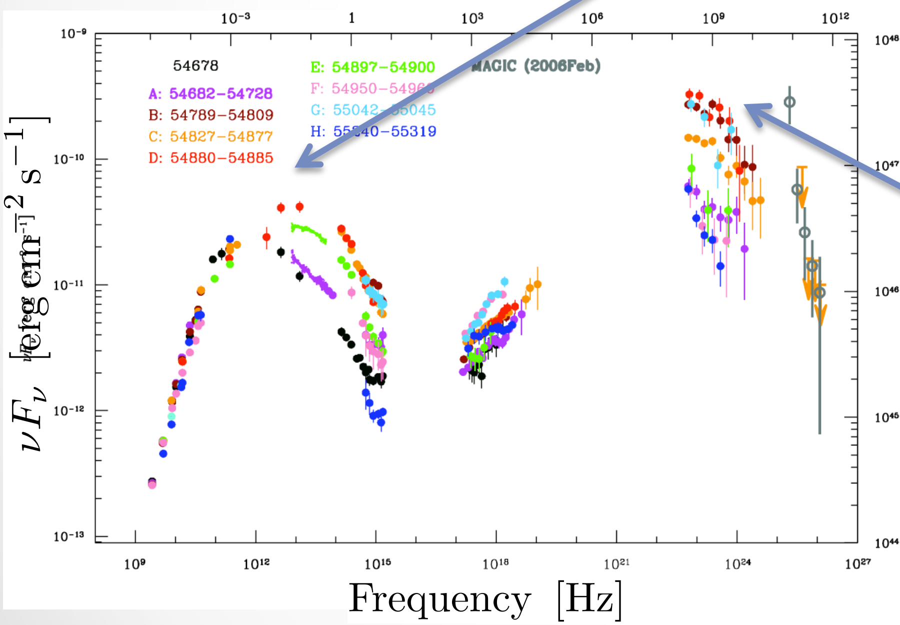

- Synchrotron emission for low energy peak
  - High polarization
- High energy peak
  - Inverse Compton
    - Synchrotron self Compton
    - External Compton
      - Accretion disk, corona
      - Broad line region
      - Dust torus

Location of the gamma-ray emission region

- The location is uncertain, but there are two main models

Close to the central engine < 1 pc

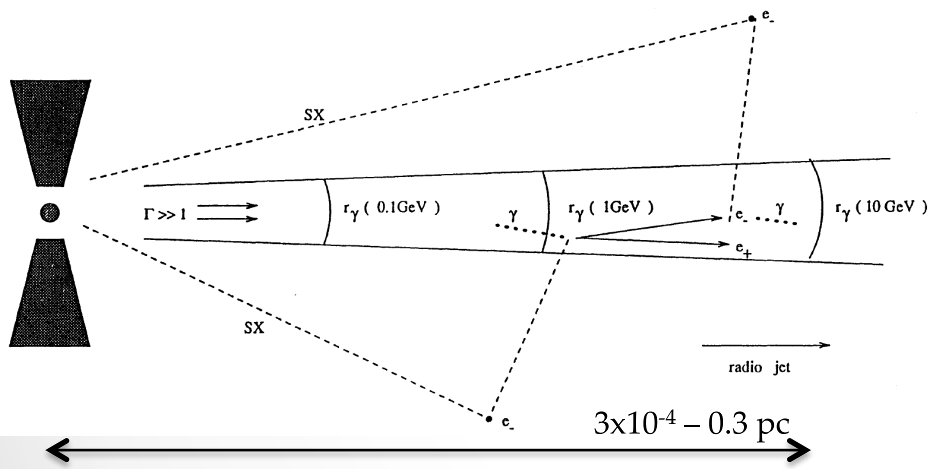

Few parsecs down the jet

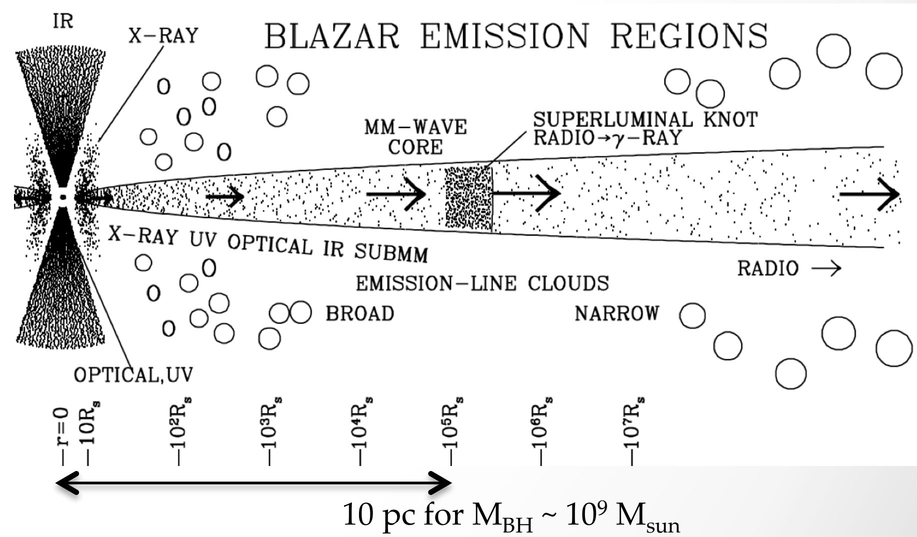

Blandford and Levinson 1995

Jorstad et al. 2001, Marscher 2006

Observational constraints

- Direct imaging is not possible
  - VLBI observations have submilliarcsecond resolution
  - Gamma-ray telescopes have ~0.3° at $E > 10$ GeV

- One alternative is to use the variability
- Correlated variations expected if the emission regions are related

- This program requires simultaneous monitoring at different bands

Previous studies

- EGRET era studies during the 1990s
  - E > 100 MeV up to 30 GeV
- Radio monitoring with single dish telescopes
- Valtaoja and Teräsranta 1995
  - Metsähovi at 22 GHz and 37 GHz
  - 70 sources
  - 202 EGRET pointings

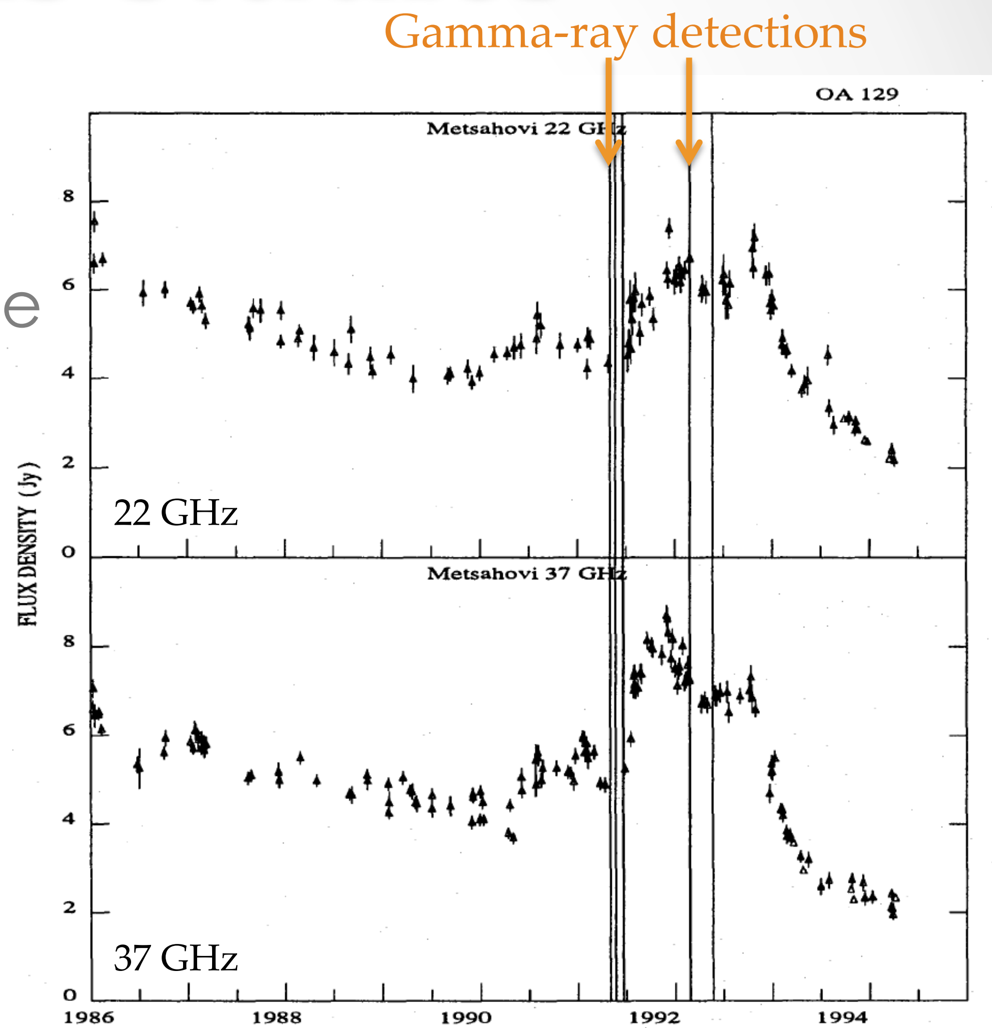

Previous studies

- EGRET + VLBA
- Jorstad et al. 2001
  - 42 sources, 10 out of 23 gamma-ray flares coincide with radio ejections

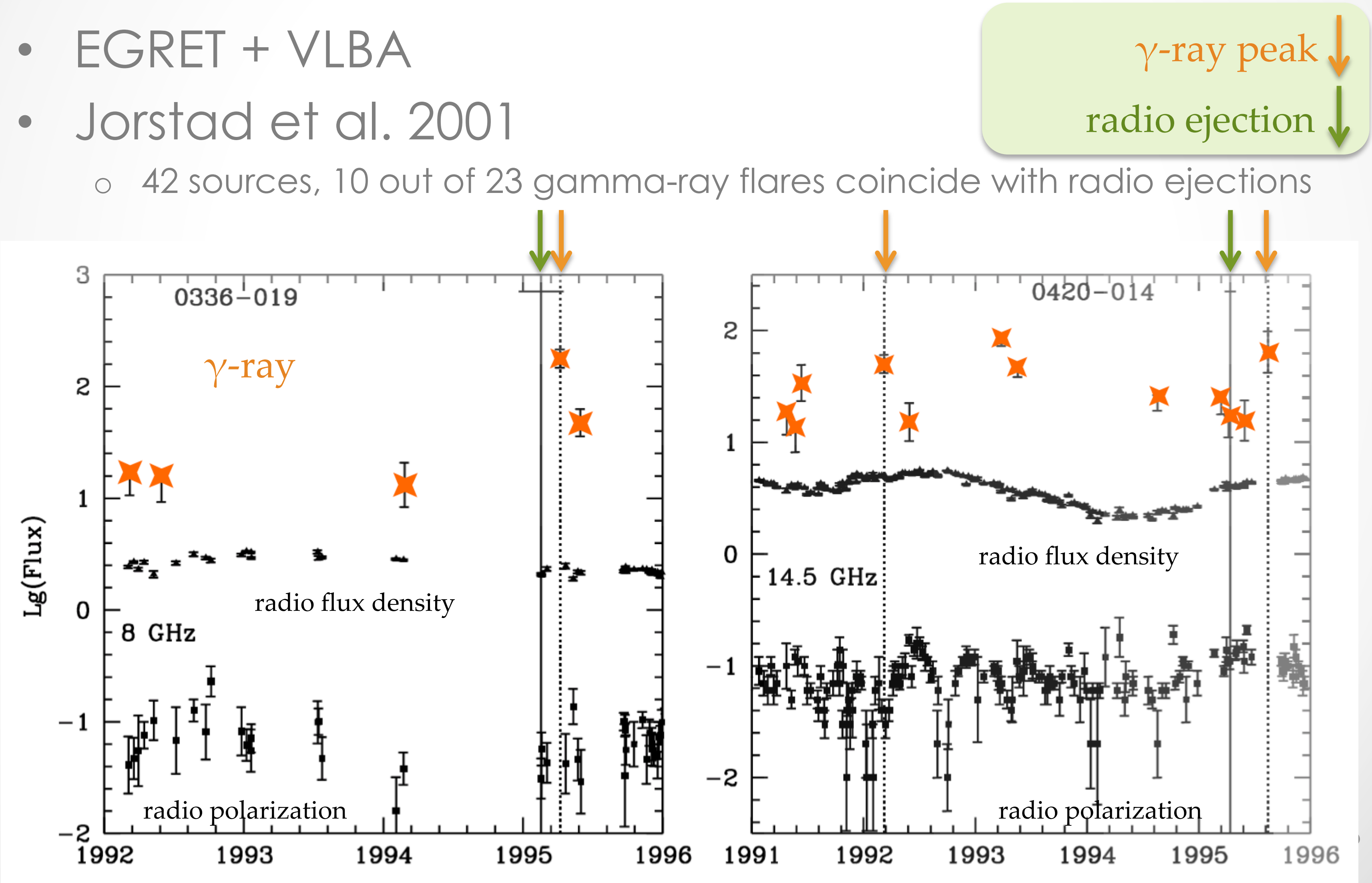

The Fermi era

- Fermi monitors the sky continuously at high energies
  - Energies from 20 MeV to 300 GeV
- A full sky map every 3 hours

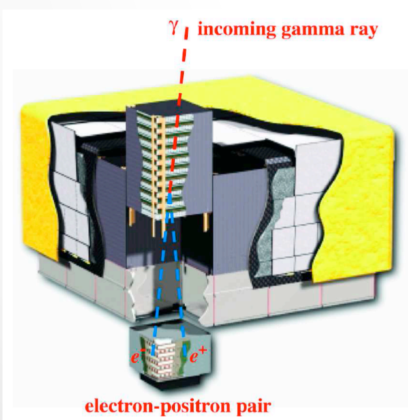

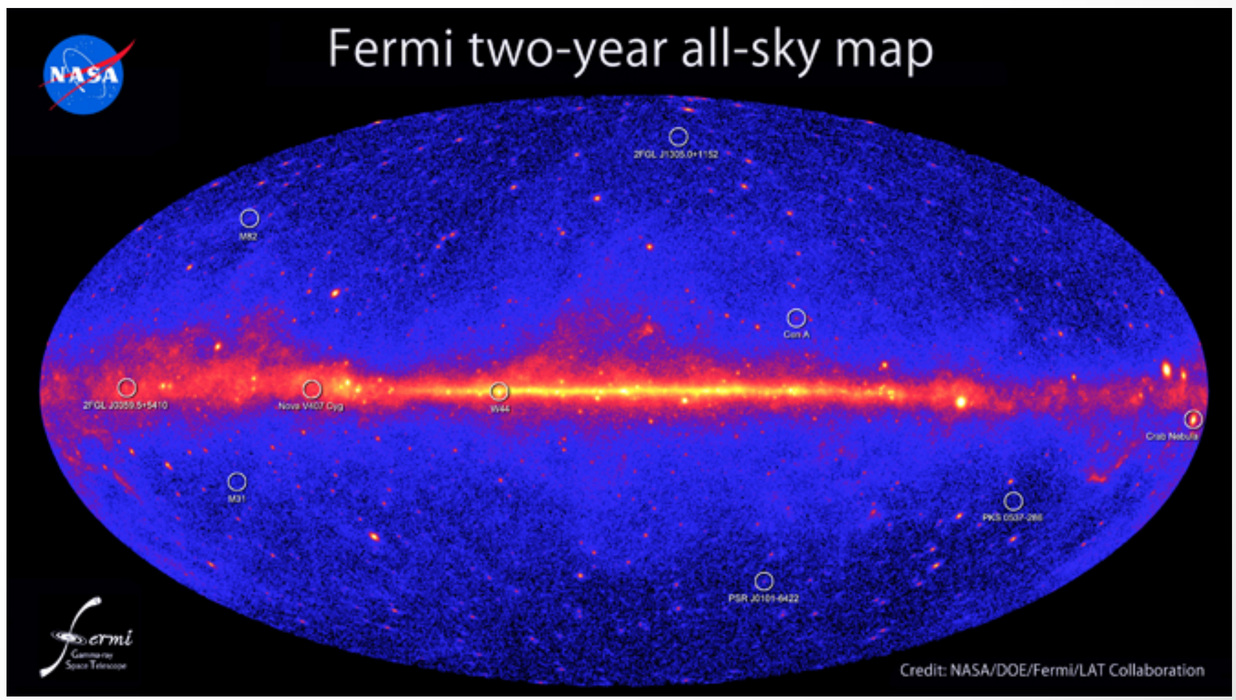

Outline

- OVRO 40 m telescope blazar monitoring program
- The cross-correlation sample
- Cross-correlation significance
- Variability in the radio band
- Cross-correlation and time lags
- The location of the gamma-ray emission site

Radio monitoring program

- Monitoring 1593 blazars
  - Including all Fermi detected
- Radio continuum
  - 15 GHz central frequency, 3 GHz bandwidth
  - 4 mJy thermal noise, ~3% typical uncertainty
- Two observation per week

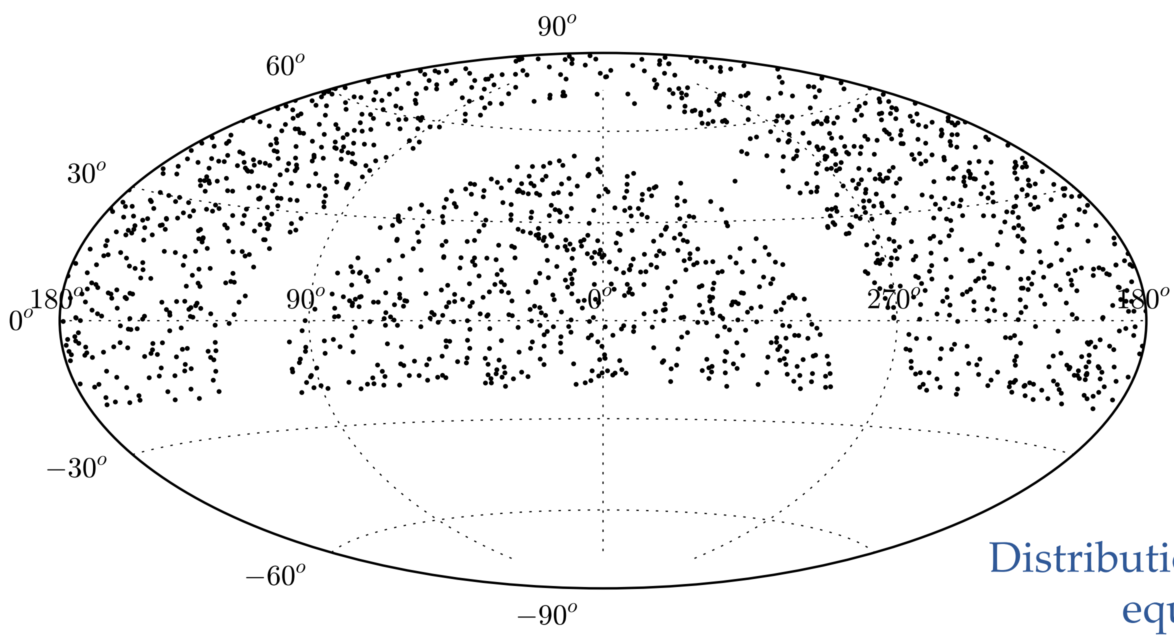

The OVRO 40 m telescope at night
by Joseph Richards

Distribution of monitored sources in equatorial coordinates

Radio monitoring

Autonomous observing + Scheduling

- Continuous unsupervised monitoring
- Maximum time on source and accurate calibration

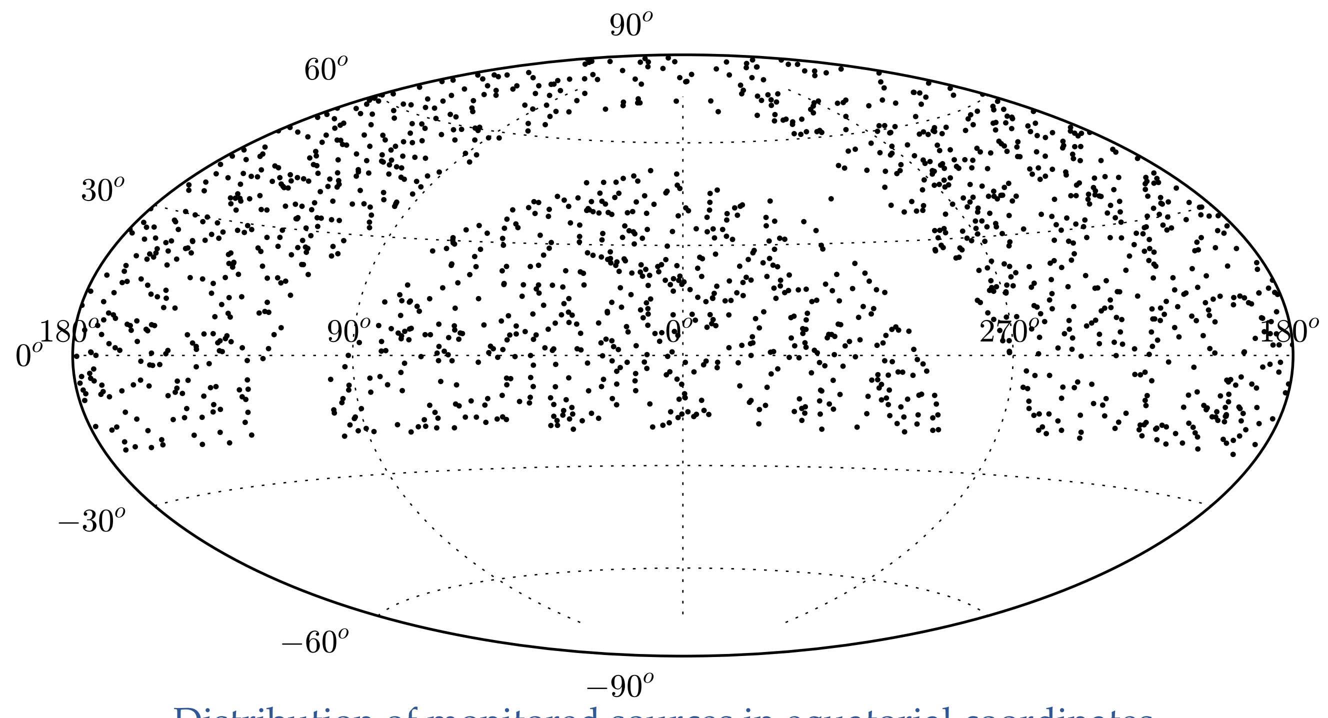

Distribution of monitored sources in equatorial coordinates

- There are many ways to observe 1593 sources
    - $1593! \sim 2\times10^{4411}$

The 40 meter in action

Radio light curves, 4 years of data
Flux density calibrators

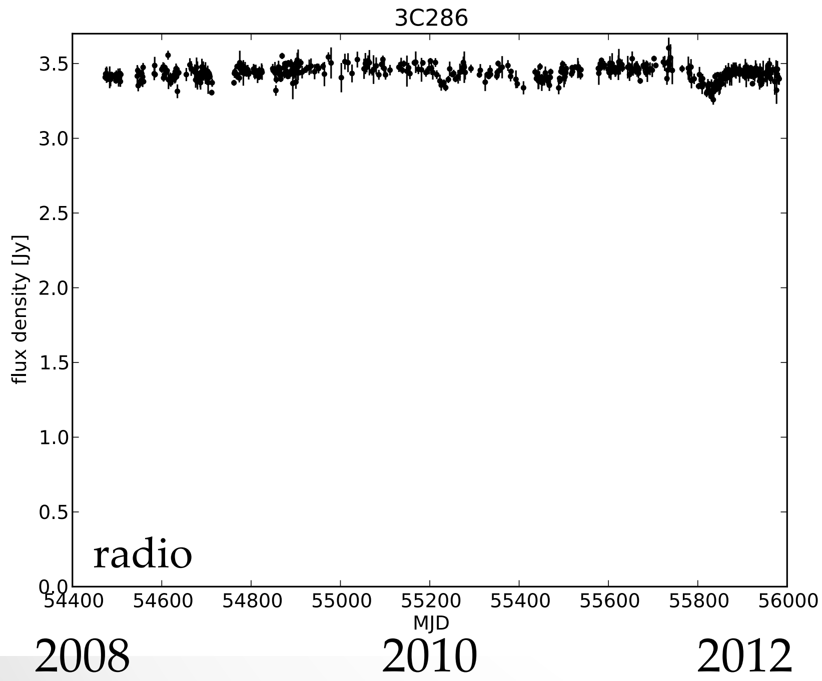

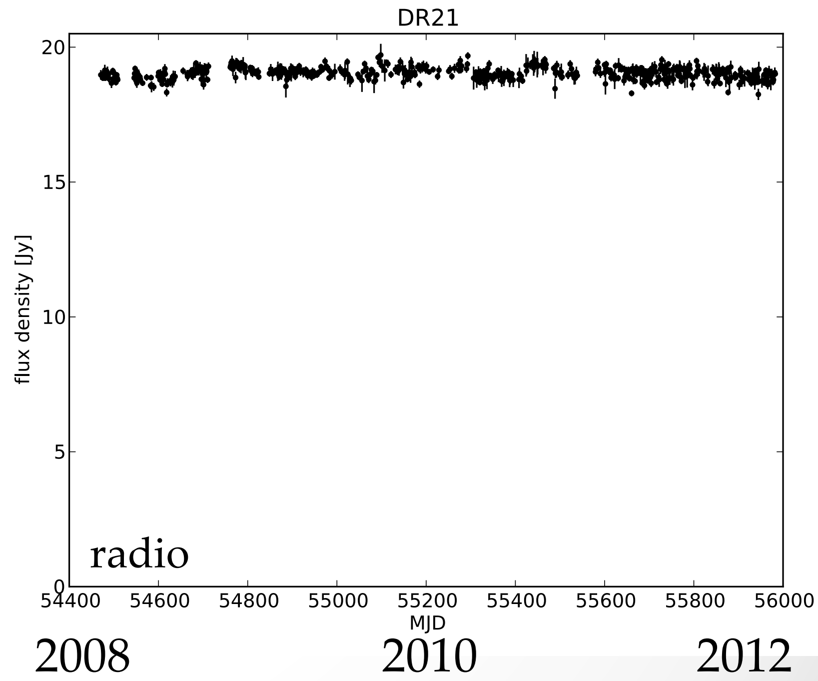

Radio light curves, 4 years of data

Some blazars

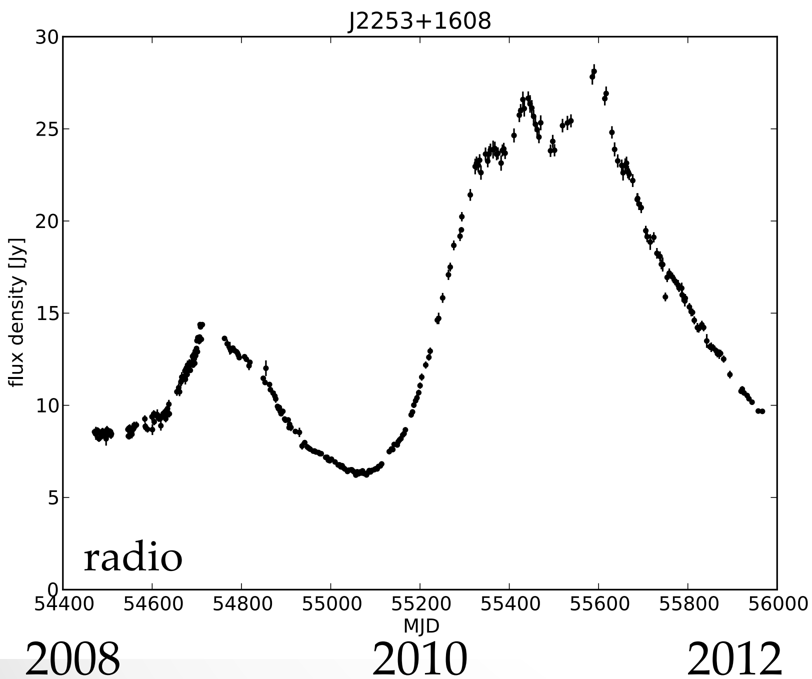

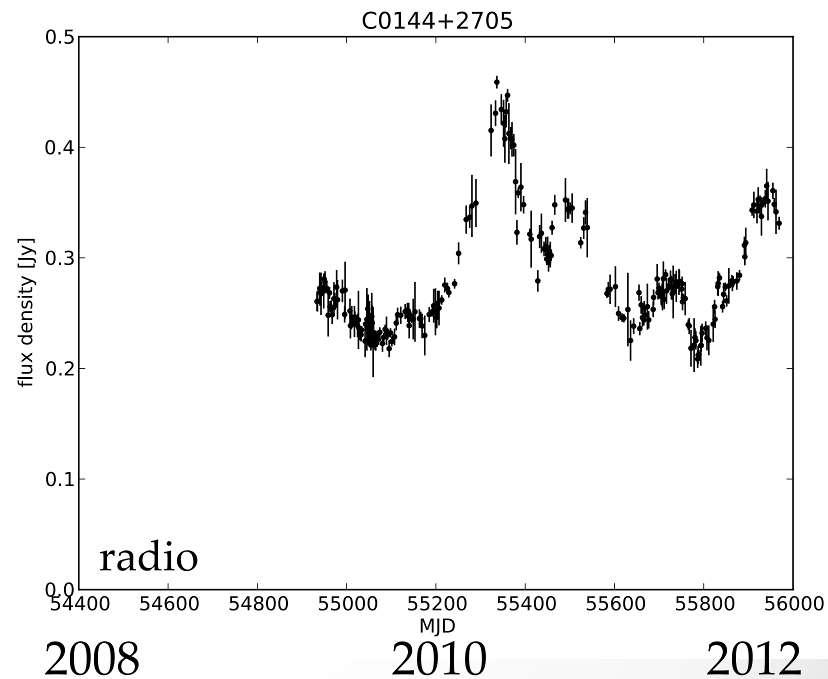

All the radio light curves

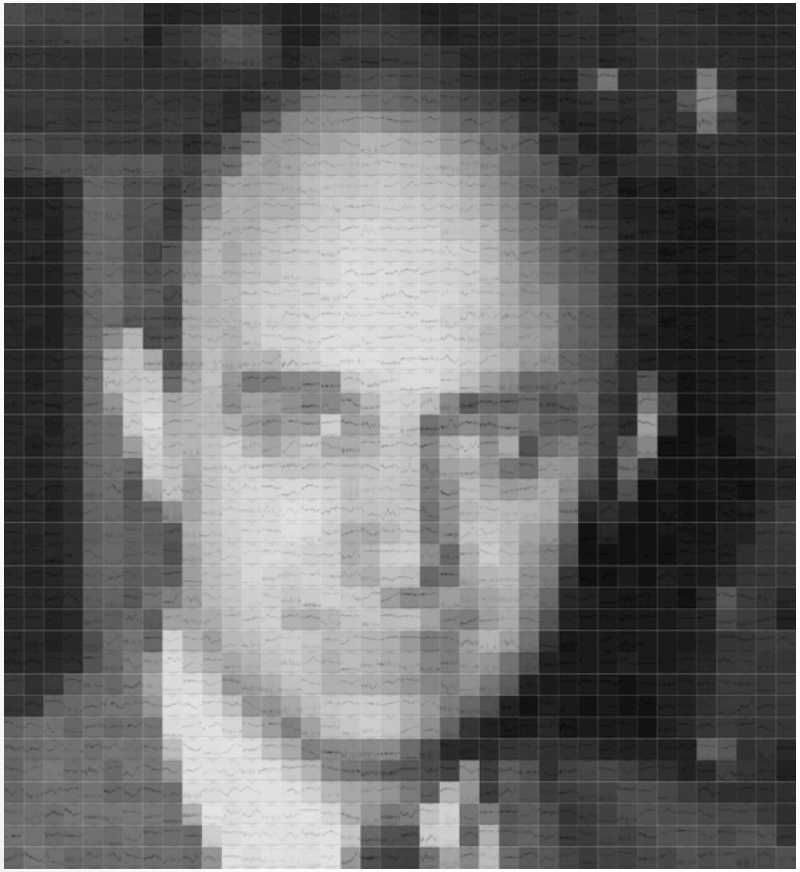

Enrico Fermi
in 1600 radio light curve pixels

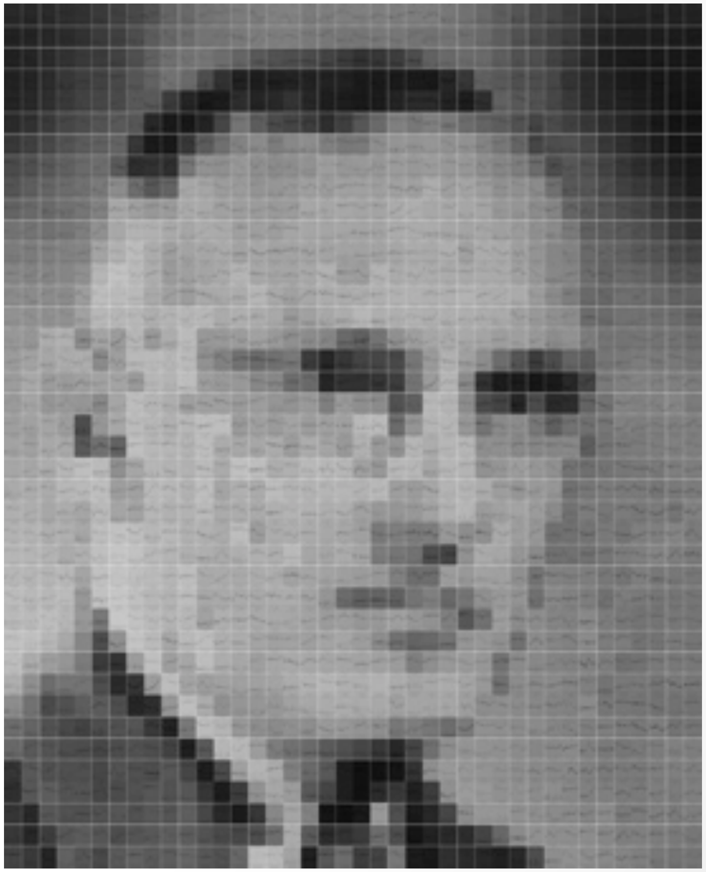

Karl Jansky
in 1600 radio light curve pixels

Cross-correlation sample

- 86 brightest gamma-ray sources
- 75 % of monthly detections in second LAT source catalog (Nolan et al. 2012)

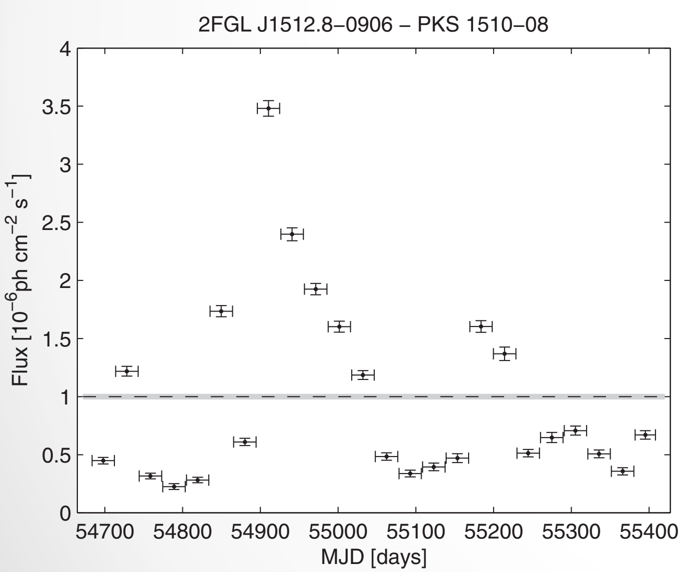

Sample monthly binned gamma-ray light curve

- Nolan et al. 2012

Table A.1: OVRO blazar monitoring program source in cross-correlation sample

OVRO name	Common name	2FGL name	RA	DEC	z	Optical Class	SED class
RBS76	KUV 00311-1938	J0033.5-1921	00:33:34.30	-19:21:34.0	0.61	BLL	HSP
J0108+0135	4C +01.02	J0108.6+0135	01:08:38.77	+01:35:00.3	2.099	FSRQ	LSP
J0112+2244	S2 0109+22	J0112.1+2245	01:12:05.82	+22:44:38.8	0.265	BLL	ISP
J0112+3208	4C 31.03	J0112.8+3208	01:12:50.33	+32:08:17.6	0.603	FSRQ	LSP
BBJ0136+3905	B3 0133+388	J0136.5+3905	01:36:32.40	+39:05:59.0	0.0	BLL	HSP
J0136+4751	OC 457	J0136.9+4751	01:36:58.59	+47:51:29.1	0.859	FSRQ	LSP
C0144+2705	TXS 0141+268	J0144.6+2704	01:44:33.56	+27:05:03.1	0.0	BLL	LSP
J0217+0144	PKS 0215+015	J0217.9+0143	02:17:48.96	+01:44:49.7	1.721	FSRQ	LSP
J0221+3556	S4 0218+35	J0221.0+3555	02:21:05.47	+35:56:13.7	0.944	FSRQ	...
3C66A	3C 66A	J0222.6+4302	02:22:39.60	+43:02:07.0	0.0	BLL	ISP
J0237+2848	4C +28.07	J0237.8+2846	02:37:52.41	+28:48:09.0	1.206	FSRQ	LSP
J0238+1636	AO 0235+164	J0238.7+1637	02:38:38.93	+16:36:59.3	0.94	BLL	LSP
J0319+4130	NGC 1275	J0319.8+4130	03:19:48.16	+41:30:42.1	0.018	Radio Gal	...
J0423-0120	PKS 0420-01	J0423.2-0120	04:23:15.80	-01:20:33.1	0.916	FSRQ	LSP
J0442-0017	PKS 0440-00	J0442.7-0017	04:42:38.66	-00:17:43.4	0.844	FSRQ	LSP
J0509+0541	TXS 0506+056	J0509.4+0542	05:09:25.96	+05:41:35.3	0.0	BLL	ISP
J0612+4122	B3 0609+413	J0612.8+4122	06:12:51.19	+41:22:37.4	0.0	BLL	...
C0719+3307	B2 0716+33	J0719.3+3306	07:19:19.42	+33:07:09.7	0.779	FSRQ	LSP
J0721+7120	S5 0716+71	J0721.9+7120	07:21:53.45	+71:20:36.4	0.0	BLL	ISP
J0725+1425	4C +14.23	J0725.3+1426	07:25:16.81	+14:25:13.7	1.038	FSRQ	LSP

Sample of the table with source properties

Gamma-ray light curves

- Data from the Fermi Gamma-ray Space Telescope
- Energy from 100 MeV to 200 GeV
- 3 years of data with 7 day time bins

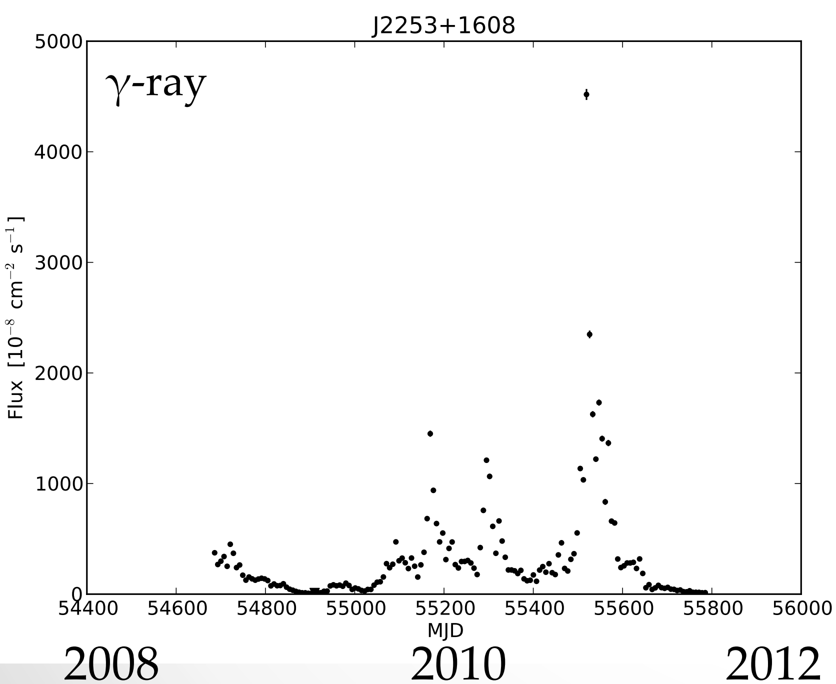

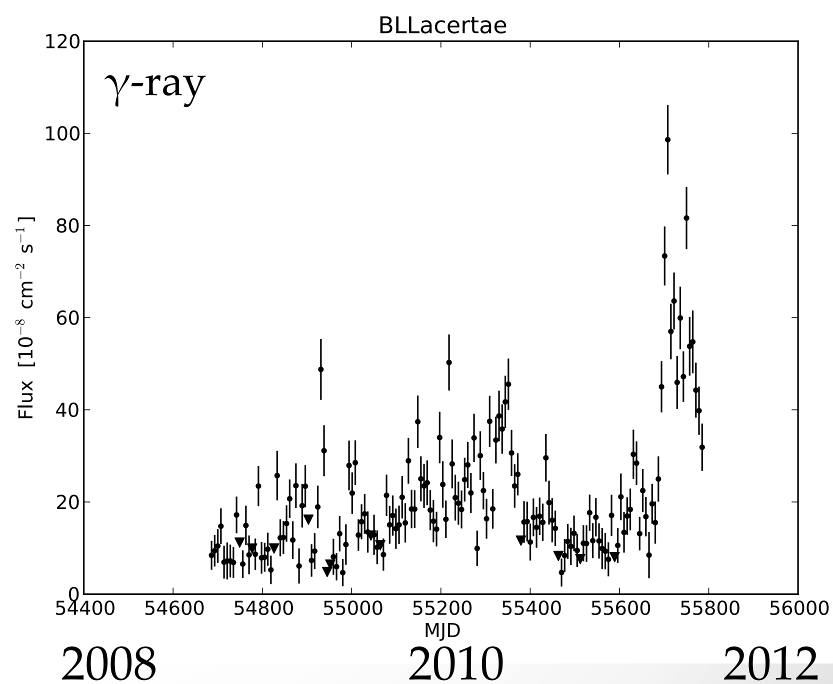

The estimation of the cross-correlation

- Cross-correlation for unevenly sampled data
  - Edelson and Krolik 1988, Welsh 1999
- This does not provide an estimate of the significance
- The significance is estimated using simulated data
  - We need a model to simulate the light curves

The significance of the cross-correlation

- Flares are common in radio and gamma-rays
- One to one identification is challenging

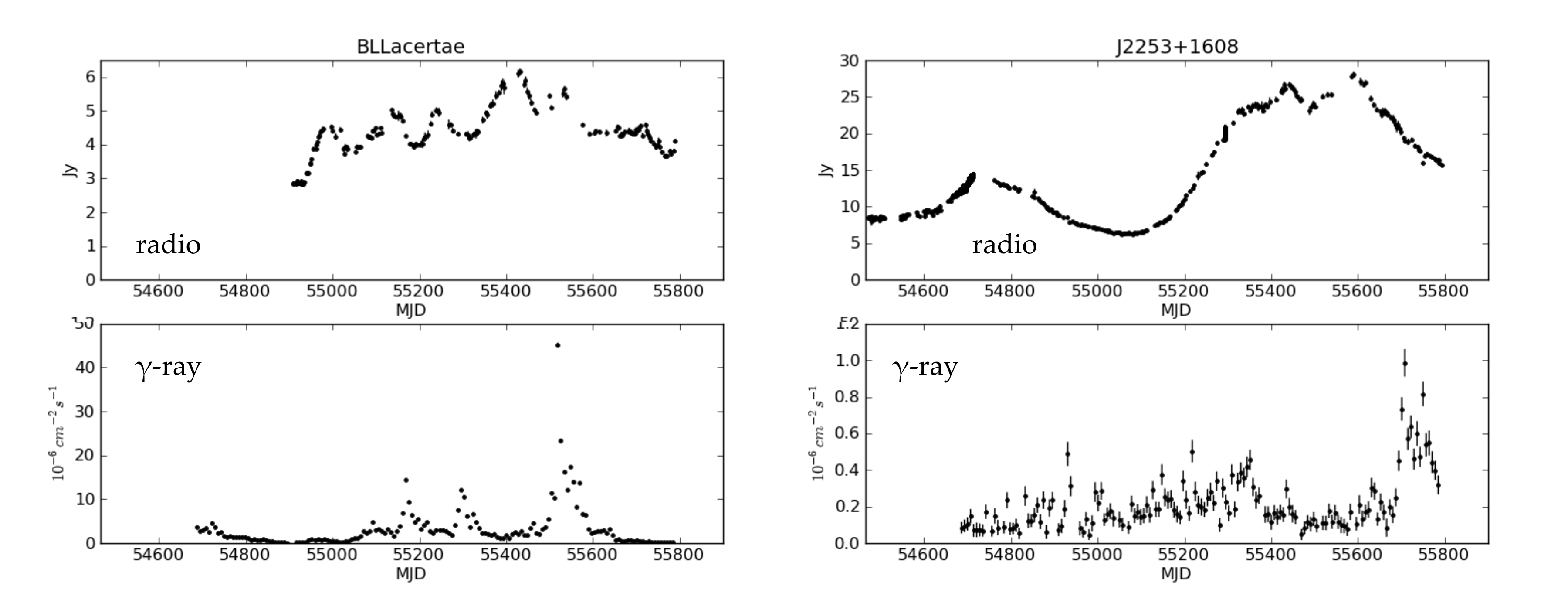

The significance of the cross-correlation

- The appearance of flares depends on the characteristics of the signal
  - Modeled with simple power law power spectral density (PSD)

$$P(\nu) \propto \frac{1}{\nu^\beta}$$

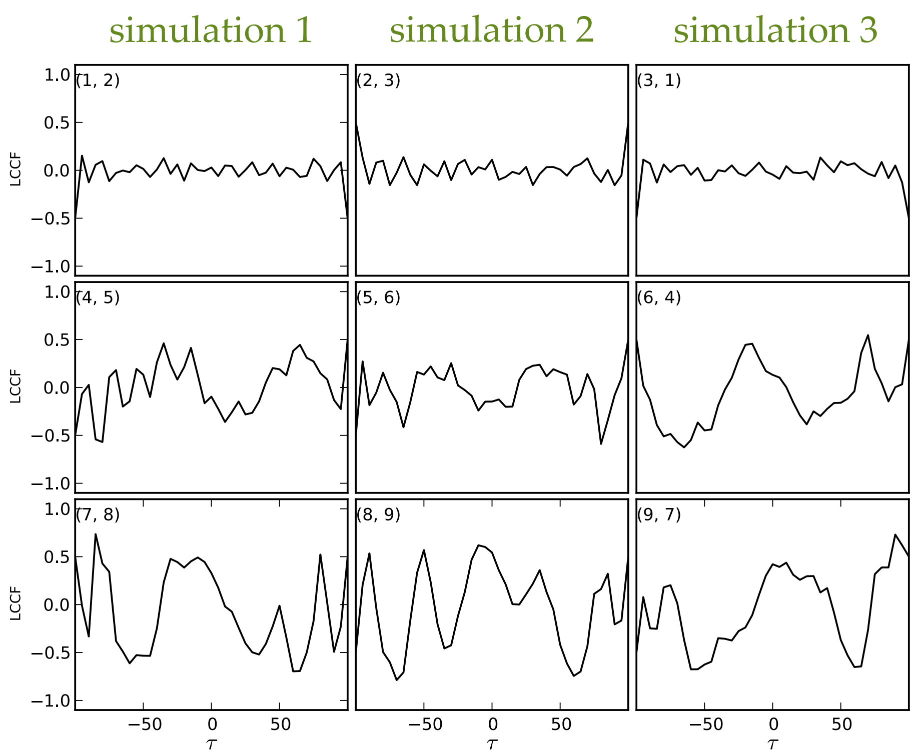

$$P(\nu) \propto \frac{1}{\nu^0}$$

$$P(\nu) \propto \frac{1}{\nu^1}$$

$$P(\nu) \propto \frac{1}{\nu^2}$$

Simulated light curves with different PSD, 3 for each case

The significance of the cross-correlation

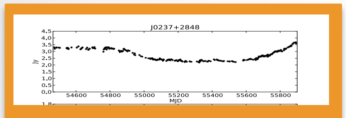

radio light curve →

PSD fit $P \sim 1 / \nu^{\beta_r}$

β_{radio}

γ-ray light curve →

PSD fit $P \sim 1 / \nu^{\beta_\gamma}$

$\beta_{\gamma-ray}$

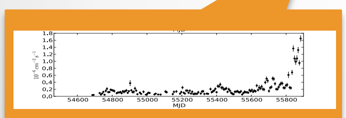

cross-correlation significance →

- Time lag
- Significance

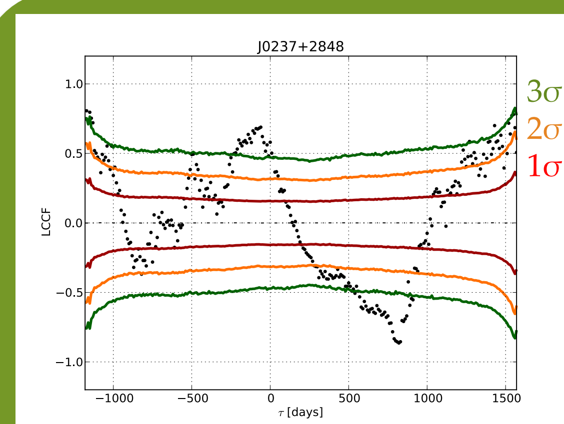

Model dependence of significance

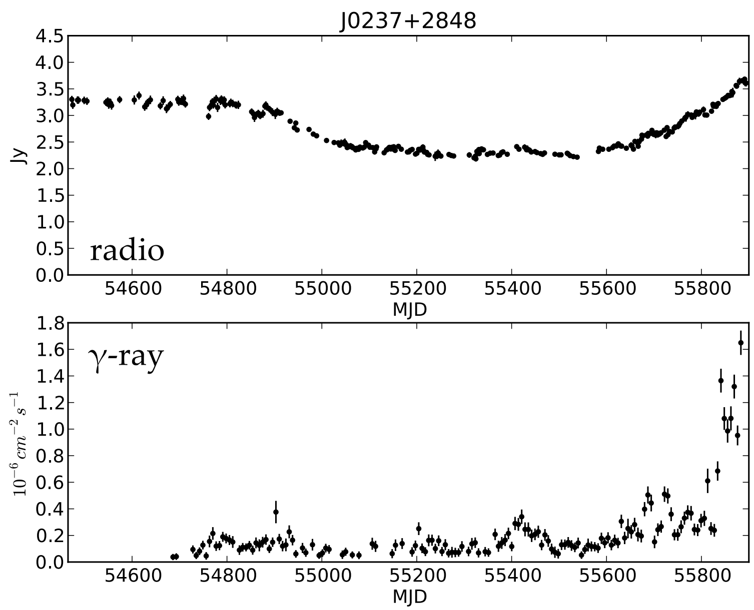

$$P(\nu) \propto \frac{1}{\nu^0}$$

$$P(\nu) \propto \frac{1}{\nu^1}$$

$$P(\nu) \propto \frac{1}{\nu^2}$$

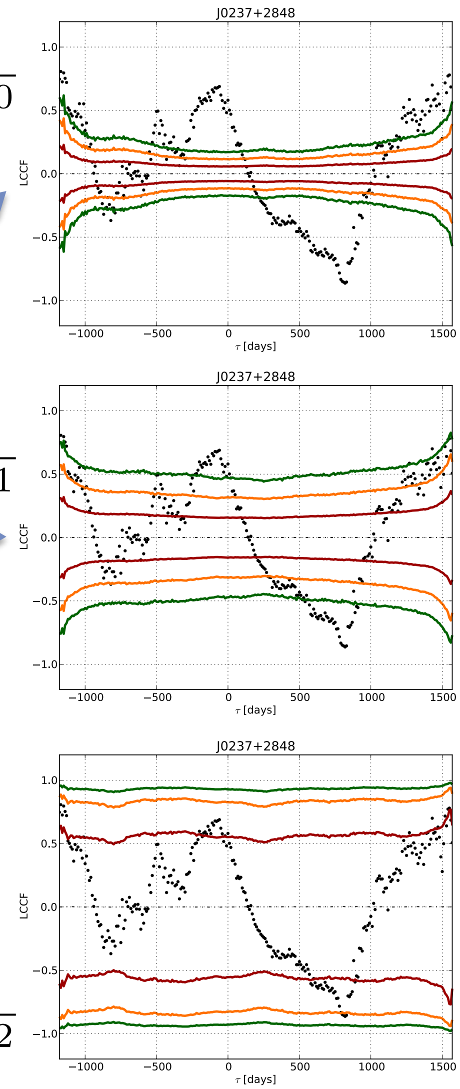

The characterization of the variability

- Variability is characterized with the PSD
- Uneven sampling is a problem
- A method was developed based on Uttley et al. 2002
- The PSD is fitted to the mean PSD of simulated data sets

$$P(\nu) \propto \frac{1}{\nu^{\beta}}$$

  - Same sampling and noise properties as data
  - Requires interpolation and sampling window function to avoid biased estimate of β, in general $\beta_{fit} < \beta_{real}$

Variability in the OVRO sample

- The method was applied to the whole OVRO sample, 1593 blazars
  - 238 have high quality fits

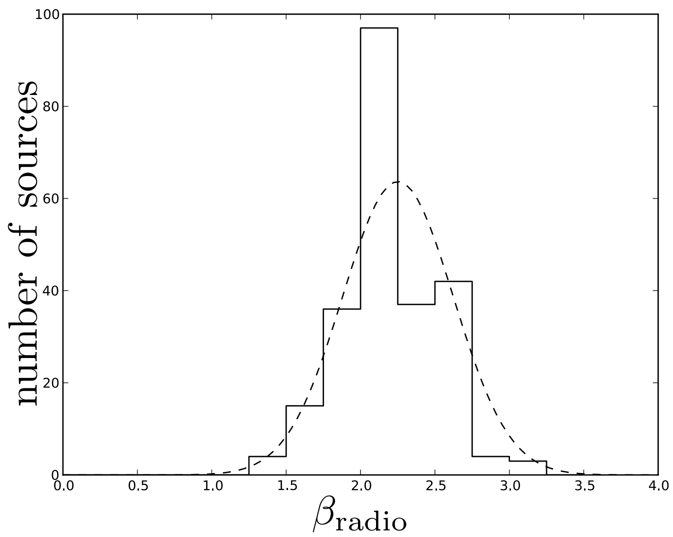

- Distribution is consistent to single value 2.25 ± 0.02
- Distributed as normal, $\mu = 2.3$ and $\sigma = 0.4$

The PSD in gamma-rays

- Fits for the PSD were possible for 23 sources
- Not consistent with single value (mean = 0.7 ± 0.1)

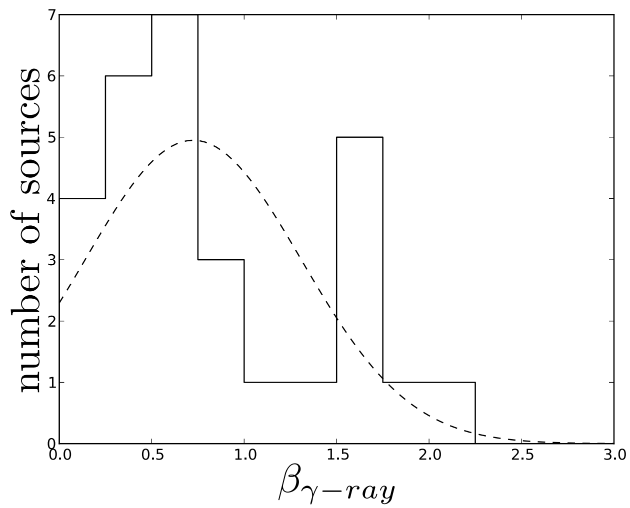

- We use mean PSD for brightest blazars, β_{gamma} = 1.6 (Abdo et al. 2010)
  - β_{gamma} = 1.7 ± 0.3 FSRQ, β_{gamma} = 1.4 ± 0.1 BL Lac

Correlations and time-lags in OVRO sample

- 41 out 86 are variable in both bands and have no flags (noise and trends)

- 13 sources have fitted PSD in radio and gamma-rays
- These have the best significance constraints

- For the other sources we use mean population values in non-constrained band of
  - $\beta_{radio} = 2.3$ and $\beta_{gamma} = 1.6$

- We set a significance limit of 97.56% (2.25σ), for which one spurious case is expected

Sources with significant correlation

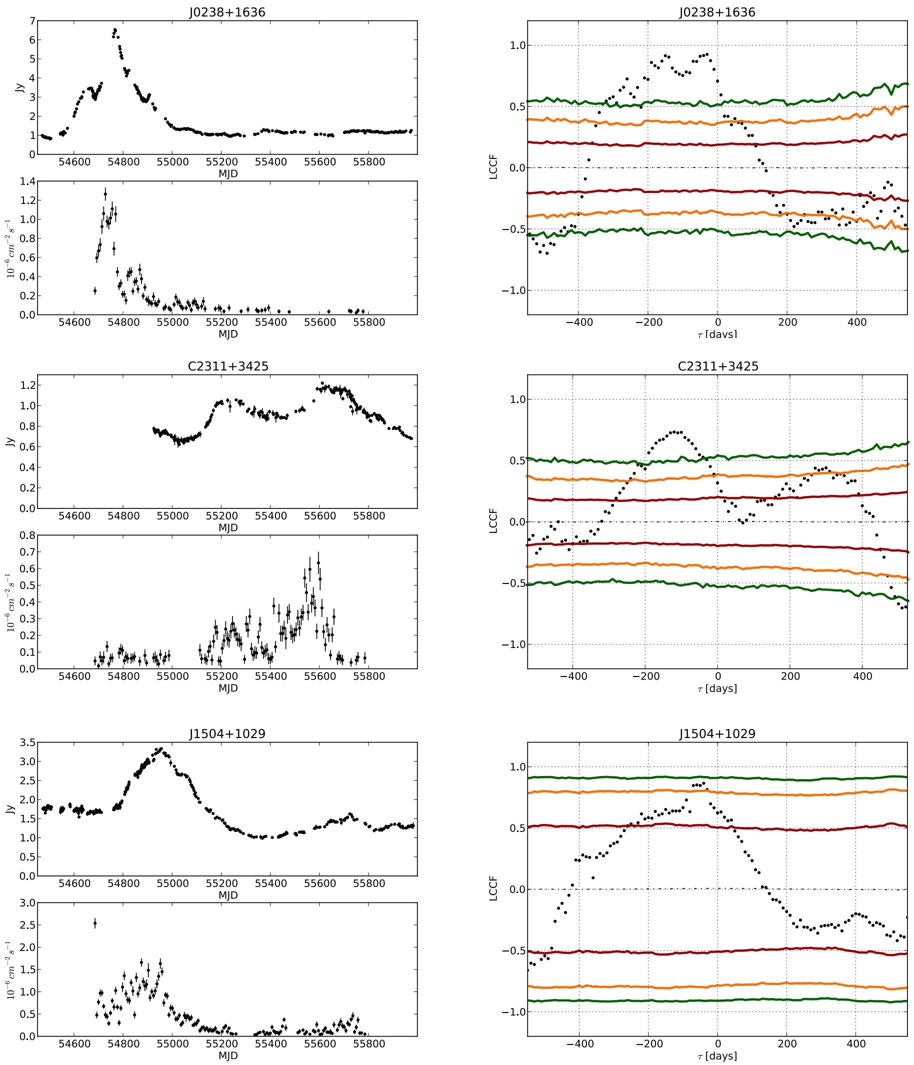

$\mathrm{AO}\,0235+164,\ \tau = -30 \pm 9\ \ \mathrm{day}$

$\tau = -150 \pm 8\ \ \mathrm{day}$

$\mathrm{B2}\,2308+34,\ \tau = -120 \pm 14\ \ \mathrm{day}$

$\mathrm{PKS}\,1502+106,\ \tau = -40 \pm 13\ \ \mathrm{day}$

Location of the gamma-ray emission region

- Only 3 out 41 are found to have significant correlation
- Radio emission lags gamma-ray variation in all cases
- An additional case, Mrk 421, is found when extending the light curve to include a period of high activity
- We can explore the relation between radio and gamma-ray emission region in these objects

Model for the correlation and time-lag

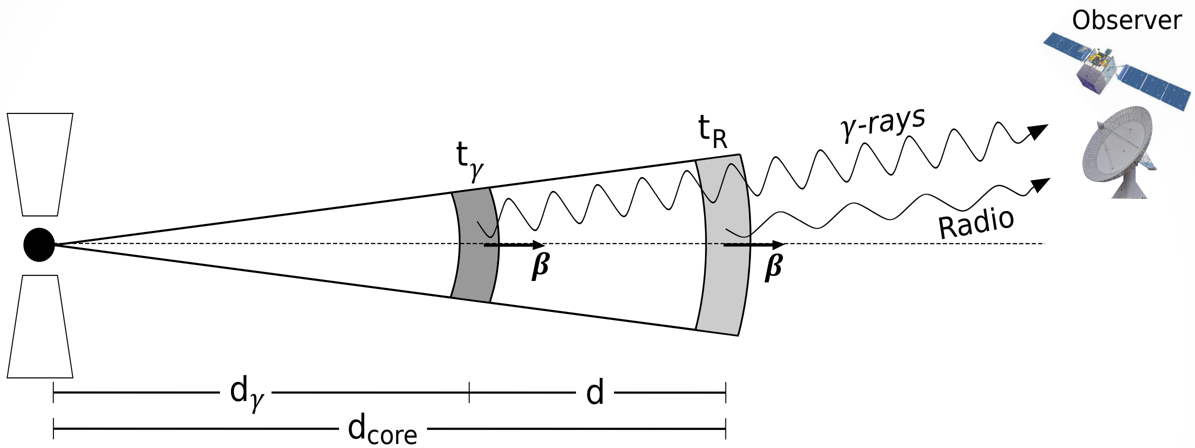

Basic model for delayed radio emission

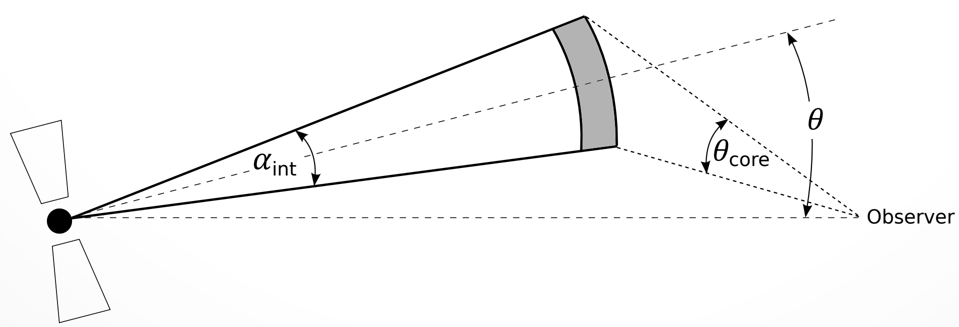

Estimation of jet properties from VLBI observations

Location of the gamma-ray emission region

Source	d [pc]	$d_{\rm core}$(coll) [pc]	$d_{\rm core}$(cone) [pc]	d_γ(coll) [pc]	d_γ(cone) [pc]
AO 0235+164, $\tau = -150 \pm 8$ day	37 ± 23	$\gtrsim 23 \pm 6$	$\gtrsim 40 \pm 11$	$\gtrsim -14 \pm 24$	$\gtrsim 3 \pm 25$
AO 0235+164, $\tau = -30 \pm 9$ day	8 ± 5	$\gtrsim 23 \pm 6$	$\gtrsim 40 \pm 11$	$\gtrsim 15 \pm 8$	$\gtrsim 32 \pm 12$
PKS 1502+106	2 ± 1	14 ± 9	24 ± 15	12 ± 9	22 ± 15

Summary

- Radio monitoring of 1593 blazars at 15 GHz
  - Large sample, continuously observed independent of gamma-ray state
- Statistical analysis
  - Variability characterization at 15 GHz for largest sample ever studied
  - Significance of cross-correlations based on measured variability properties
- 3 sources out of 41 show significant correlation
  - An additional object shows correlated variability when extended light curves are used
- In all significant cases:
  - Radio emission lags gamma-ray variations.
  - Indication that gamma-ray emission is produced upstream of radio
- In one case gamma-rays originate parsecs away from the central engine